

Towards the glueball spectrum from unquenched lattice QCD.

E. Gregory^{a,d} A. Irving^b B. Lucini^c C. McNeile^d A. Rago^e C. Richards^b E. Rinaldi^{f,g}

^a*Department of Physics, University of Cyprus, P.O. Box 20357 1678 Nicosia, Cyprus*

^b*Theoretical Physics Division, Dept. of Mathematical Sciences, University of Liverpool, Liverpool L69 7ZL, UK*

^c*Department of Physics, College of Science, Swansea University, Singleton Park, Swansea SA2 8PP, UK*

^d*Bergische Universität Wuppertal, Gausstr. 20, D-42119 Wuppertal, Germany*

^e*School of Computing & Mathematics, University of Plymouth, Plymouth, PL4 8AA, UK*

^f*SUPA, School of Physics and Astronomy, University of Edinburgh, Edinburgh EH9 3JZ, UK*

^g*Kobayashi-Maskawa Institute for the Origin of Particles and the Universe (KMI), Nagoya University, Nagoya 464-8602, Japan*

E-mail: gregory@uni-wuppertal.de, aci@liverpool.ac.uk,
b.lucini@swansea.ac.uk, mcneile@uni-wuppertal.de,
antonio.rago@plymouth.ac.uk, cmr@liverpool.ac.uk,
e.rinaldi@sms.ed.ac.uk

ABSTRACT: We use a variational technique to study heavy glueballs on gauge configurations generated with 2+1 flavours of ASQTAD improved staggered fermions. The variational technique includes glueball scattering states. The measurements were made using 2150 configurations at 0.092 fm with a pion mass of 360 MeV. We report masses for 10 glueball states. We discuss the prospects for unquenched lattice QCD calculations of the oddballs.

Contents

1	Introduction and motivation	1
2	Details of the lattice QCD calculation	3
3	Results	7
4	Classifying the glueballs into continuum angular momentum states	8
5	Conclusions and future prospects	13

1 Introduction and motivation

Nothing is more symbolic of the difficulty of solving QCD, than the fact that, while glueballs are central to the understanding of non-perturbative QCD, there is currently no definite experimental evidence for their existence. After much work the glueball spectrum [1] in quenched QCD was mapped out by Morningstar and Peardon and collaborators [2, 3]. Results for higher spin glueballs have been reported by Meyer and Teper [4, 5] (see also [6]).

There has been much less work done on studying the effect of sea quarks on the glueball masses [7–10]. Glueball calculations suffer from a severe problem with the signal to noise ratio that requires high statistics. Also, some of the more sophisticated algorithms used in quenched QCD calculations that improve the signal to noise error, do not work for unquenched calculations [5, 11].

The properties of glueballs can be elucidated by studying the experimental decay and production of flavour singlet mesons. Some of these analyses find that the glueball degrees of freedom have similar masses to the quenched glueballs [12], while others find very different masses [13, 14]. For example, one analysis [13] of the decay properties of the 0^{-+} states suggested that large unquenching effects moved the quenched 0^{-+} glueball from 2.6 GeV to 1.4(1) GeV, close to the experimental mass of the $\eta(1405)$ meson.

Some have argued (e.g. [15]) that there is an additional state over the two expected $\bar{q}q$ mesons in the 0^{++} flavour singlet mesons: $f_0(1370)$, $f_0(1500)$, and $f_0(1710)$. The mass of the 0^{++} glueball inferred from quenched QCD [2] is 1730(50)(80) MeV. This could be important in understanding the above mesons if one assumes that unquenching effects in the 0^{++} glueball are small. Other groups, e.g. [14], have argued that unquenching of the 0^{++} may be large and that the mass in QCD is close to the σ . There is also some controversy as to whether the $f_0(1370)$ is a real meson state [16], although it is listed in the Particle Data Group (PDG) summary tables. Lattice calculations will eventually have to deal with the decays of the f_0 mesons and possible coupling of the $f_0(980)$ and $f_0(600)$.

The mixing of the glueball degrees of freedom with flavour singlet mesons has meant that many lattice groups [17–21] have been studying the ρ meson and P-wave states such

as the $a_1(1260)$, $b_1(1235)$ meson using a variety of techniques so as to understand how to deal with resonances in lattice QCD calculations.

So, in summary, there are no hadrons where glueball degrees of freedom have been confirmed. Looking to the future, there are ongoing experiments that are searching for glueball degrees of freedom, such as the BES III experiment [22]. The BES III experiment has preliminary [23] results for two new states with masses close to the 0^{+-} and 1^{+-} quenched glueball masses. In 2018, the PANDA experiment [24] will search for heavy glueballs with masses under 5.4 GeV. In particular they will look for oddball glueballs with exotic J^{PC} quantum numbers (0^{+-} , 2^{+-} , 1^{-+} , 0^{--} and 3^{-+}) which are not allowed in quark models for quark-antiquark mesons. In a quenched QCD calculation, Morningstar and Peardon [2] found two glueballs with exotic $J^{PC} = 2^{+-}$ and 0^{+-} with masses 4140(50)(200) MeV and 4740(70)(230) MeV respectively. As we review later, other quenched glueball studies have not seen these states [25].

One motivation for studying glueballs heavier than 3 GeV is that there could be reduced mixing with flavour singlet quark states. There have been speculations that there are no further, or a reduced number of, light meson states above 3.1 GeV [26, 27], based on string breaking of the heavy quark potential. Swanson [28] critiques the use of screened potentials in hadron spectroscopy. The heaviest light meson in the PDG summary table [29] is the $f_6(2510)$ with a mass of 2.469 GeV. It is possible that there may be no experiments capable of producing light mesons beyond 2.5 GeV. It could be that heavier mesons made from light quarks have large widths, so it becomes difficult to extract the masses from experiment. Even though the signal to noise ratio is worse for heavier glueballs than for light glueballs, it would simplify lattice QCD calculations if heavier glueballs do not mix with quark degrees of freedom, because it would be simpler to identify a pure glueball state. For glueball masses above 3 GeV, there is the possibility that the glueballs may mix with charmonium states. However, Page [27] suggests that the mixing between charmonium states and glueballs will be small, because the charm quark is heavy and hence it is difficult to excite a charm loop.

The hadron spectrum collaboration [30] has computed the spectrum of excited mesons and baryons, although typically at a single lattice spacing and heavy quark masses. They don't report any meson masses above 2.8 GeV. Studying such masses is already an impressive achievement, and it is not clear whether they can investigate the meson spectrum at even higher masses.

Hagedorn conjectured that the density of light hadrons goes like $e^{m/T}$ where m is the mass of the light hadrons and T is a constant [31, 32]. Cohen and Krejcirik have recently reviewed [33] the evidence that the number of light hadrons agrees with the Hagedorn conjecture.

There may be indirect ways of determining whether there exist light mesons in the regime 3 to 6 GeV, using information from thermodynamic studies. For example, the hadron resonance gas model (HRGM) is used in the phenomenology of heavy ion experiments and has successfully reproduced some results from lattice QCD calculations at non-zero temperature. The HRGM depends on the number of mesons and baryon states. Typically the meson and baryon states listed in the PDG are used, however Chatterjee et al. [34] have studied a different density of states, with mesons with masses higher than those listed

β	$L^3 \times T$	am_l	am_s	N_{cfg}	N_{traj}	r_0/a
7.095	$32^3 \times 64$	0.00775	0.031	2150	12900	5.059(10)

Table 1. Summary of the parameters of the ensemble used in this calculation. We use the same convention for the quark masses as used by the MILC collaboration. The configurations used are taken every 6 trajectories.

in the PDG. Majumder and Muller use the results from lattice QCD [35, 36] calculations with the HRGM to claim the existence of new light resonances [37]. Megias et al. [38] study the effects of the additional hadrons predicted by the quark model on the results of the HRGM.

The PANDA experiment is performing some Monte Carlo studies of glueball production using glueball decay widths of 10 MeV [39]. It will be important to check some of these speculations about the density of light mesons and the mixing of glueball and charmed hadrons.

Oddball glueballs will not mix with light mesons with non-exotic J^{PC} quantum numbers. Even if the heavier glueball states do not mix with quark degrees of freedom, there is the possibility that the glueballs decay to other glueballs. The calculation reported here explicitly includes glueball scattering states to check for this.

In [10], the results for 0^{++} , 0^{-+} , and 2^{++} were presented on the gauge configurations also used in this study¹. A powerful variational code was developed in [40] that included two glueball scattering states and was used to study glueballs in $SU(N)$ quenched QCD. In this paper, we use this code to extend the study in [10] to look at glueballs with new J^{PC} . We will mostly study the glueballs with J^{PC} quantum numbers not studied in the earlier work [10].

There are a number of reviews on the theory of glueballs [41, 42], lattice QCD calculations of glueballs [43], and experimental searches [44] for glueball degrees of freedom.

2 Details of the lattice QCD calculation

The unquenched lattice QCD calculations used the ASQTAD improved staggered fermion action [45, 46] and the one link Symanzik improved gauge action [47]. These are the same actions used by the MILC collaboration [48]. The configurations were described in one paper on glueball masses [10] and one on the masses of the η and η' mesons [49]. The parameters of the calculation are shown in Tab. 1. The lattice spacing a was determined from the r_0/a parameter calculated from the heavy quark potential and the value of r_0 (0.4661 fm) determined by the HPQCD collaboration [50] on the configurations generated by the MILC collaboration [48].

Glueball masses were extracted with a variational calculation. The variational technique used in this work was described in [40]. Here we provide a brief summary. The basis states for the variational procedure are made from operators that transform under an irreducible representation of the cubic lattice group and have specified parity and charge

¹In particular, this work uses the set of configurations referred to as the *fine ensemble* in [10].

conjugation quantum numbers. The irreducible representations of the cubic group, which is the discrete rotational symmetry group of the lattice, are conventionally called A_1 , A_2 , E , T_1 and T_2 . Representations A_1 and A_2 have dimension 1, E has dimension 2 and T_1 and T_2 have dimension 3. Below, we show how the continuum spin can be obtained from mass eigenstates transforming according to an irreducible representation of the cubic group.

On a given timeslice, a single glueball operator with well-defined rotational quantum number is a prescribed linear combination of traced Wilson loops of a given shape. Eigenstates of parity are obtained by considering the starting linear combination and the reflected one, while eigenstates of charge conjugations are given by the real part ($C = 1$) and the imaginary part ($C = -1$) of that combination. In our calculations, we considered operators containing shapes from length 4 to length 10. In addition to single glueball operators, the basis states include two-gluon scattering states (which involve products of two basic shapes) and bi-torelon operators (products of two loops winding in a compact spatial direction; note that these operators are not necessarily straight lines). In order to keep the number of operators under control, we limited the number of single glueball operators to at most 30. The shapes we included in our calculations are those that contribute in as many channels as possible and, barring shapes that for symmetry reasons do not contribute to given channels, the same basis shapes have been used for all the quantum number assignments. Other constraints imposed on the basis operators were that the variational basis must contain shapes of all lengths and that a given shape can contribute at most once in a given channel. This allowed us to include a broad range of shapes and lengths in our basis. A Mathematica program systematically constructed the basis operators with the requested constraints. A summary of the number of operators we have used for each quantum number assignment is reported in Fig. 1. Additional operators were generated by an improved blocking algorithm [51]. We used 6 different blocking and smearing levels, which implies that for each channel our basis is 6 times larger than the number of operators quoted in Fig. 1.

Consider two basis operator Φ_α and Φ_β . In the lattice QCD calculations the correlators between operators separated by time t are computed and define the correlation matrix

$$\tilde{C}_{\alpha\beta}(t) = \sum_{\tau} \langle 0 | \Phi_\alpha^\dagger(t + \tau) \Phi_\beta(\tau) | 0 \rangle \quad . \quad (2.1)$$

The masses and amplitudes of glueball states can be extracted from the generalized eigenvalue problem on the measured correlation matrix: the optimal operators (i.e. those that almost coincide with pure states) are the eigenvectors of

$$\bar{C}(\bar{t}) = \tilde{C}^{-1}(0) \tilde{C}(\bar{t}) \quad . \quad (2.2)$$

These interpolating operators are a linear sum of the basis vectors:

$$\tilde{\Phi}_i(t) = \sum_{\alpha} v_{\alpha}^i \Phi_{\alpha}(t) \quad . \quad (2.3)$$

The mass of the state is extracted by cosh fits of the correlation matrix in the optimal basis:

$$\bar{C}_{ii}(t) = |c_i|^2 \cosh(m_i t - N_T/2) \quad , \quad (2.4)$$

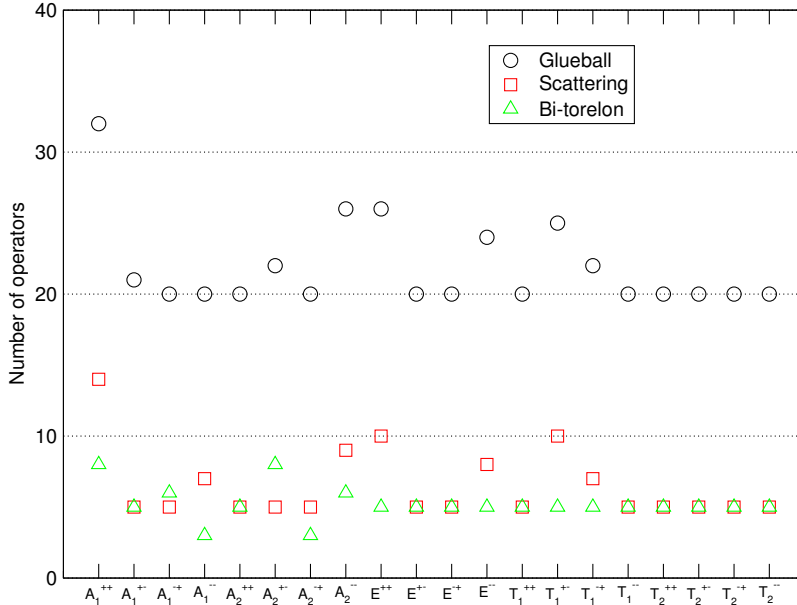


Figure 1. Number of basis operators (before blocking and smearing) in each channel, for single glueballs, scattering states and bi-torelon states.

where N_T is the length of the lattice in the time direction and the cosh functional form is a consequence of the usual exponential decay in a lattice with periodic boundary condition in the time direction.

In general, glueball correlators are very noisy and this limits the usefulness of numerical correlators to short time separations. However, although Eq. (2.4) is only valid at large t , if the overlap with an Hamiltonian state is almost perfect, it is possible to extract a reliable value for the mass at short time separation, since the decay is largely dominated by a single state. For this to be true, a careful construction of the variational basis is paramount. Whether an optimal state $\tilde{\Phi}_i$ is a good approximation of the Hamiltonian eigenstates can be checked by looking at the value of the overlap $|c_i|^2$: the closer this number is to one from below (with one being the unitarity limit), the better is the variational calculation. In addition, it is important to estimate the contributions to the mass coming from scattering and torelon states. For the eigenstate corresponding to a true spectral mass, these contaminations must be absent. The contribution of scattering and torelon states for a given optimal state can be resolved by looking at the relative length of its projection onto the space spanned respectively by the scattering and bi-torelon basis operators. A summary of the resulting relative projections is shown in Fig. 2. For the lightest states extracted in each symmetry channel we show the relative projection onto the different types of basis operators (single glueballs, scattering and bi-torelon operators).

We do not include any fermionic scattering states in this calculation. Fu has recently reported [52] preliminary results for the decay width of the 0^{++} σ into $\pi\pi$. New techniques for calculating the masses of scalar mesons using lattice QCD have been developed [53, 54].

The results come from bin sizes of 50 configurations. We have checked for autocorrela-

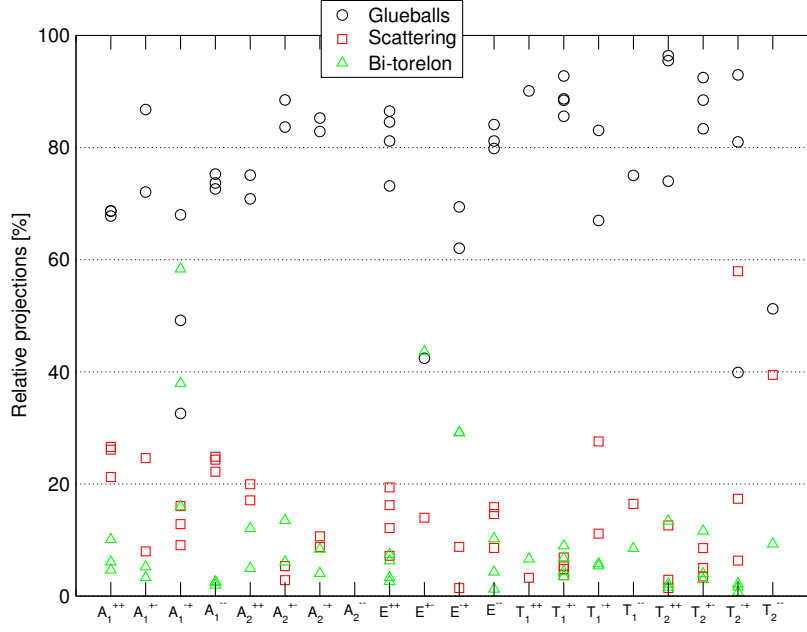


Figure 2. Summary of the projections relative to the subspace spanned by different types of basis operators for the lightest states in the spectrum.

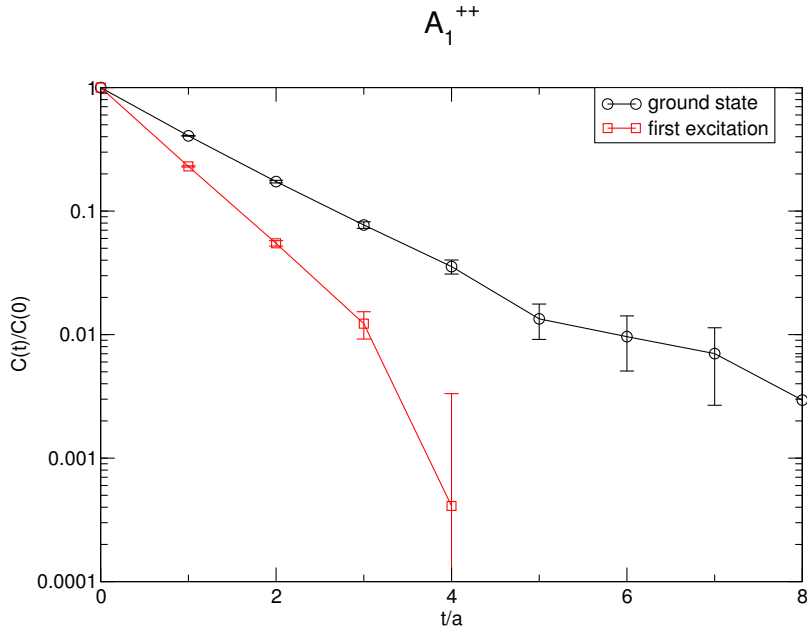


Figure 3. Normalized correlator in log scale for the two lightest states in the spectrum of the 0^{++} channel.

tion effects by choosing different binning blocks down to 5 configs. We found no evidence for correlations.

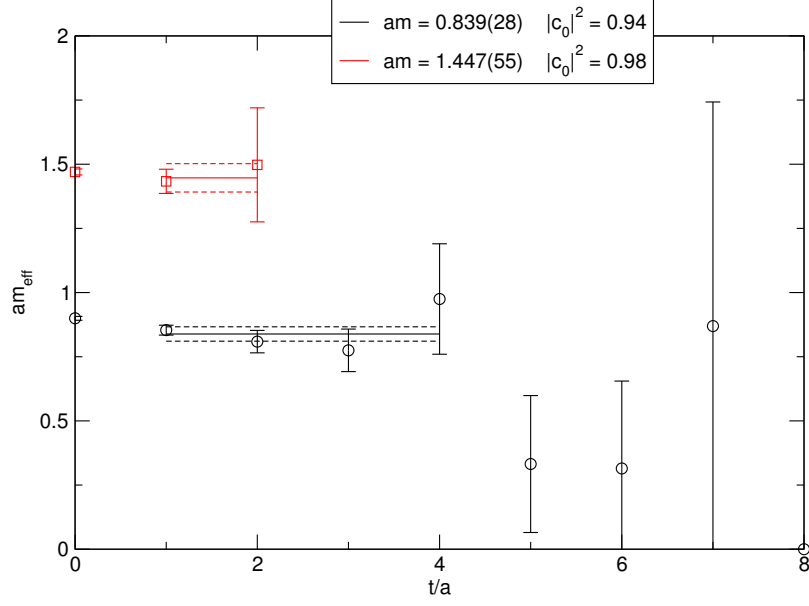


Figure 4. Effective mass plateaux for ground state (circles) and the first excitation (squares) in the 0^{++} channel. The fitted values are shown with solid lines (the dashed lines represent one standard deviation).

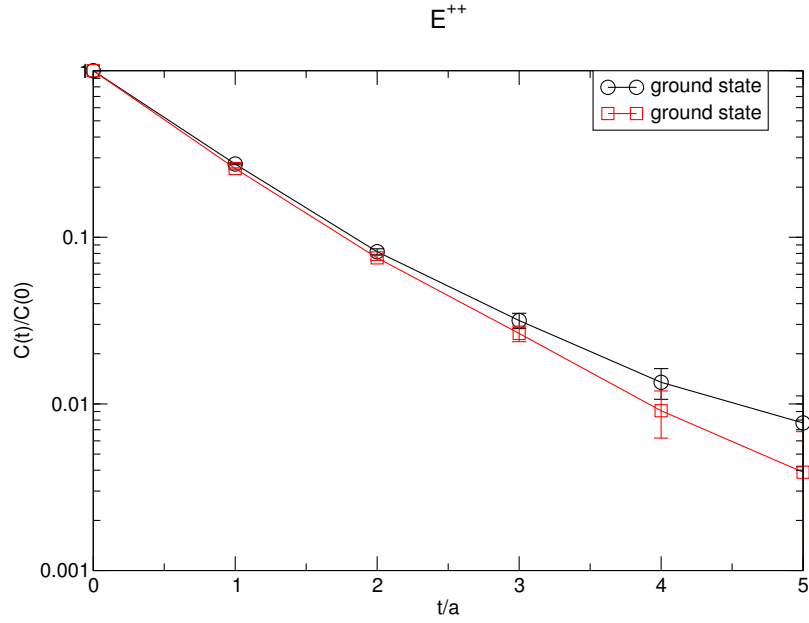


Figure 5. Normalized correlator in log scale for the lightest state in the spectrum of the E^{++} channel.

3 Results

We reduced the variational correlators Eq. (2.1) truncating the diagonal matrix Eq. (2.2) to the 5 highest eigenvalues (corresponding to the 5 lowest masses). The diagonal correlators

are fitted to the fit model in Eq. (2.4). The functional form is a good approximation if the overlap $|c_i|^2 \sim O(1)$ and the $\chi^2/\text{dof} \sim O(1)$. All the states we were able to measure have $0.65 < |c_i|^2 < 1.1$, with order 0.1 errors and $0 < \chi^2/\text{dof} < 1.25$.

The correlator for the lightest glueball (the A_1^{++} channel, which in the continuum encodes the scalar 0^{++} glueball) and its first excitation is shown in Fig. 3 on a logarithmic scale. The effective mass plateaux of these two states with the corresponding estimate of the fitted masses from the fit in Eq. (2.4) are reported in Fig. 4. A similar plot for the E^{++} channel corresponding to the continuum tensor glueball is shown in Fig. 5. For the A_1^{++} , we have investigated alternative variational calculations that include only some of the subsets of our operators (only single glueball operators or only scattering and torellon operators). We note that in both cases the mass of the ground state is the same within errors. This phenomenon is different from what happens in pure gauge, where for sets excluding single glueball operators the ground state mass is roughly twice the mass of the ground state one finds when single glueball are included in the variational basis [40]. This might be due to the explicit breaking of centre symmetry in the presence of dynamical fermions. Although the coupling of glueball states and single torellon states was found to be negligible in [8], it is possible that it becomes more relevant closer to the chiral limit. To investigate this coupling systematically would require variational calculations with a basis including single torellon operators at various quark masses close to the chiral limit. A similar calculation is beyond the scope of this paper.

In Fig. 6 we plot the glueball masses for each lattice representation. A summary of the spectrum is reported in Tab. 2. We define glueball states as those with an overlap of at least 65% onto the single glueball operators.

We also include the results from Chen et al. [3] from a quenched lattice QCD calculation in the continuum limit. Fig. 6 does not show any significant unquenching effects, although the continuum limit of the unquenched results should be taken before a definitive statement can be made.

4 Classifying the glueballs into continuum angular momentum states

Each of the states comes from an operator that is a linear combination of ones in the variational basis. The projection on the 3 subsets can be used to identify single glueball states from scattering or bi-torellon states. Only the A_2^{--} , T_2^{-+} and T_2^{--} channels had O(40)% overlap with the scattering subset of operators. Also only the A_1^{-+} and E^{+-} channels had contaminations of O(40)% overlap with bi-torellons. We find that the channels A_1^{++} , A_1^{+-} , A_1^{--} and T_1^{-+} had contaminations with scattering states of between 20% and 40%. The A_1^{-+} and E^{-+} channels had bi-torellons contaminations between 20% and 40%.

Identification of the spin of glueball states on the lattice is non-trivial. Continuum spin representations break down into lattice representations at finite lattice spacing. In Tab. 3 the continuum spin representations are broken down into lattice representations.

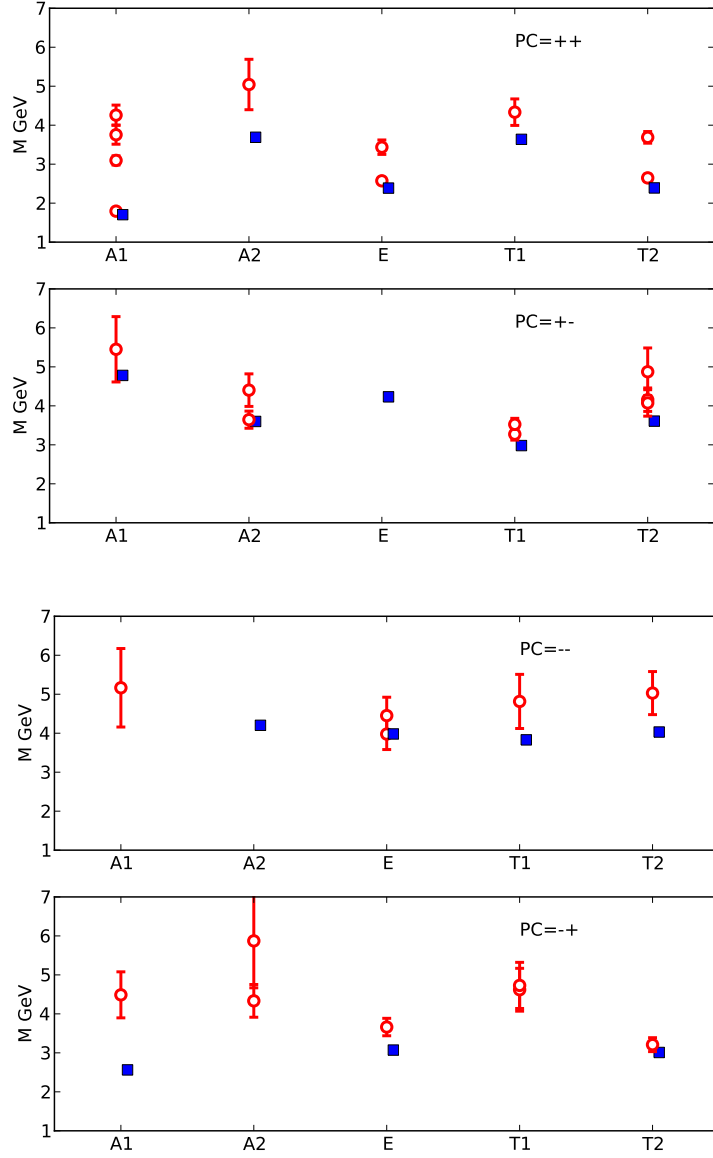


Figure 6. Glueball masses for the different lattice representations. Open circles refer to results obtained in this study, filled squares are quenched results from [3].

Ch.	$t_{\min} - t_{\max}$	am	$ c_0 ^2$	χ^2/dof	mix_G	mix_S	mix_T
A_1^{++}	1-5	0.839(28)	0.94(3)	0.23	0.6874	0.2661	0.0466
A_1^{++*}	1-5	1.447(55)	0.98(5)	0.48	0.6779	0.2611	0.0609
A_1^{+++}	1-4	1.75(11)	0.88(10)	0.91	0.6865	0.2124	0.1010
A_1^{+++*}	1-5	1.99(12)	1.16(14)	0.91	0.6727	0.2055	0.1217
A_1^{+-}	1-5	2.55(39)	0.99(38)	0.31	0.7207	0.2461	0.0331
A_1^{-+}	1-6	1.30(4)	0.89(3)	0.15	0.3257	0.0908	0.5835
A_1^{-+*}	1-5	1.57(8)	0.73(6)	0.79	0.4919	0.1284	0.3797
A_1^{--*}	1-5	2.10(28)	0.76(20)	0.97	0.6800	0.1605	0.1595
A_1^{--}	1-4	2.41(47)	0.81(39)	0.64	0.7263	0.2486	0.0251
A_2^{++}	1-4	1.94(13)	0.99(13)	0.30	0.7509	0.1995	0.0495
A_2^{+-}	1-4	2.36(30)	1.08(33)	0.06	0.7086	0.1708	0.1206
A_2^{+-}	1-5	1.70(10)	0.76(8)	0.48	0.8366	0.0284	0.1350
A_2^{+-*}	1-3	2.06(10)	0.79(15)	0.41	0.8850	0.0535	0.061
A_2^{-+}	1-4	2.03(20)	0.66(13)	0.56	0.8528	0.1067	0.0405
A_2^{-+*}	1-4	2.74(56)	0.97(60)	1.03	0.8528	0.1067	0.0405
A_2^{--}	1-5	2.32(25)	0.98(25)	1.10	0.5526	0.3905	0.0569
E^{++}	1-5	1.202(32)	0.86(3)	0.97	0.8117	0.1622	0.0261
E^{+++}	1-5	1.606(87)	0.89(8)	0.44	0.8457	0.1213	0.0330
E^{+-}	1-4	2.42(40)	0.98(39)	0.01	0.4243	0.1398	0.4359
E^{-+}	1-5	1.42(6)	0.76(5)	0.76	0.4243	0.1398	0.4359
E^{-+*}	1-3	1.71(10)	0.81(8)	0.57	0.6943	0.0143	0.2914
E^{--}	1-5	1.86(19)	0.71(13)	1.1	0.7984	0.1586	0.0430
E^{--*}	1-5	2.08(22)	0.83(18)	0.92	0.8411	0.1464	0.0126
T_1^{++}	1-4	2.03(16)	0.92(15)	0.90	0.9011	0.0327	0.0662
T_1^{+-}	1-5	1.530(71)	0.86(6)	0.45	0.8870	0.0689	0.0441
T_1^{+-*}	1-4	1.65(7)	0.87(6)	0.26	0.9277	0.0371	0.0352
T_1^{-+}	1-5	2.16(26)	0.89(23)	0.24	0.6700	0.2759	0.0541
T_1^{-+*}	1-5	2.21(28)	0.85(24)	1.15	0.8308	0.1114	0.0578
T_1^{--}	1-5	2.25(32)	0.96(31)	0.33	0.7504	0.1645	0.0851
T_2^{++}	1-4	1.238(43)	0.92(4)	0.63	0.9640	0.0144	0.0216
T_2^{++*}	1-4	1.723(70)	0.92(6)	0.85	0.9551	0.0291	0.0159
T_2^{+-}	1-4	1.90(16)	0.83(13)	0.99	0.8336	0.0504	0.1160
T_2^{+-*}	1-4	2.28(29)	0.94(26)	0.92	0.9249	0.0350	0.0401
T_2^{-+}	1-4	1.50(8)	0.76(6)	0.93	0.8101	0.1736	0.0163
T_2^{-+*}	1-5	1.69(12)	0.90(10)	0.28	0.3989	0.5795	0.0217
T_2^{--}	1-4	2.35(26)	1.07(26)	0.91	0.5124	0.3946	0.0930

Table 2. Spectrum on the ensemble of Tab. 1. For each state we were able to extract a signal, we show the parameters of the fit with Eq. (2.4) and the relative projection of the mass eigenstate on the different subsets of operators (mix_G , mix_S , mix_T). Good overlaps $|c_0|^2 \sim \mathcal{O}(1)$ and χ^2/dof are shown.

J	A_1	A_2	E	T_1	T_2
0	1	0	0	0	0
1	0	0	0	1	0
2	0	0	1	0	1
3	0	1	0	1	1
4	1	0	1	1	1

Table 3. Subduced representations $J \downarrow \mathcal{G}_O$ of the octahedral group up to $J = 4$. This table illustrates the spin content of the irreducible representations of \mathcal{G}_O in terms of the continuum J .

J^{PC}	Mass MeV			
	Unquenched This work	Quenched		
		M&P	Ky	Meyer
0^{-+}		2590(40)(130)	2560(35)(120)	2250(60)(100)
2^{-+}	3460(320)	3100(30)(150)	3040(40)(150)	2780(50)(130)
0^{-+}	4490(590)	3640(60)(180)		3370(150)(150)
2^{-+}				3480(140)(160)
5^{-+}				3942(160)(180)
0^{--} (exotic)	5166(1000)			
1^{--}		3850(50)(190)	3830(40)(190)	3240(330)(150)
2^{--}	4590(740)	3930(40)(190)	4010(45)(200)	3660(130)(170)
2^{--}				3.740(200)(170)
3^{--}		4130(90)(200)	4200(45)(200)	4330(260)(200)
1^{+-}	3270(340)	2940(30)(140)	2980(30)(140)	2670(65)(120)
3^{+-}	3850(350)	3550(40)(170)	3600(40)(170)	3270(90)(150)
3^{+-}				3630(140)(160)
2^{+-} (exotic)		4140(50)(200)	4230(50)(200)	
0^{+-} (exotic)	5450(830)	4740(70)(230)	4780(60)(230)	
5^{+-}				4110(170)(190)
0^{++}	1795(60)	1730(50)(80)	1710(50)(80)	1475(30)(65)
2^{++}	2620(50)	2400(25)(120)	2390(30)(120)	2150(30)(100)
0^{++}	3760(240)	2670(180)(130)		2755(30)(120)
3^{++}		3690(40)(180)	3670(50)(180)	3385(90)(150)
0^{++}				3370(100)(150)
0^{++}				3990(210)(180)
2^{++}				2880(100)(130)
4^{++}				3640(90)(160)
6^{++}				4360(260)(200)

Table 4. Glueball masses with J^{PC} assignments. The column M&P reports results from Morningstar and Peardon [2] from quenched QCD. The column labelled Ky is the data from Chen et al. [3]. Meyer's results are from [25].

Meyer and Teper [25, 55] have developed systematic techniques to classify glueball masses into spins. Dudek et al. [56] have stressed the importance of correctly identifying lattice representations with spin in the charmonium system. Here, we use the simplest spin identification. We identify the $J = 0$ state with the A_1 , and $J = 1$ state with the T_1 representation, and $J = 2$ states with almost degenerate T_2 and E representations. For $J = 2$ and $J = 3$ states we take a weighted average of the masses in the component lattice representations.

Morningstar and Peardon [2] found glueball states with 0^{-+} (ground and excited), and 2^{-+} quantum numbers. In the $PC = -+$ sector in Fig. 6 there are two almost degenerate levels in the E and T_2 representations that could come from a $J = 2$ state. There is one level in the A_1 representation which is relatively isolated and so is expected to couple to 0^{-+} states. There are also degenerate levels in the A_2 , and T_1 representations that could be 3^{-+} . This would be interesting, because 3^{-+} is an exotic quantum number, however, because there is no signal in T_2 representation, this state is not included in the summary tables.

In the $PC = --$ sector in Fig. 6, the errors are large because the masses are very heavy. Morningstar and Peardon [2] found glueball states with 1^{--} , 2^{--} , and 3^{--} . Here we see evidence for a 2^{--} state with near-degenerate masses in the E and T_2 channel. The results in Fig. 6 are not consistent with 3^{--} , because there is no signal in the A_2 channel. There is also a hint of a signal for the spin exotic 0^{--} state in the A_1 representation, but unfortunately with large errors.

For the operators with $PC = ++$ in Fig. 6, there is potentially a rich mixture of states. Morningstar and Peardon [2] found glueball states with 0^{++} (ground and excited), and 2^{++} . There are two 0^{++} states in the A_1 channel. There are two almost degenerate states in the E and T_2 channel that would correspond to a 2^{++} state in the continuum. The agreement of the effective masses for these two lattice states, together with the fitted masses using Eq. (2.4) is shown in Fig. 7. The mass degeneracy between these two channels is supposed to be exact in the continuum limit, when the full three-dimensional rotational symmetry is dynamically restored.

There is potentially a 4^{++} appearing in the A_1 , E , T_1 , and T_2 representations. There is also a potential 3^{++} state in the A_2 representation, but there is no hint of degenerate states in the T_1 and T_2 representations.

In quenched QCD, Morningstar and Peardon [2] found glueball states with $J^{PC} = 3^{+-}$, 1^{+-} , 2^{+-} , and 0^{+-} . The summary of the masses in Fig. 6 doesn't show a signal in the E^{+-} , so our results are inconsistent with an exotic 2^{+-} state. There is evidence for states with $J^{PC} = 3^{+-}$, 1^{+-} , and 0^{+-} .

In Tab. 4 we summarise our assignments for J^{PC} quantum numbers to the glueball masses from operators, and compare with other results in the literature from quenched QCD calculations. Note that the calculations by Meyer and Teper [25, 55] used the string tension to determine the lattice spacing, however Morningstar and Peardon [2] and Chen et al. [3] used r_0 . This may cause a systematic difference in the results. Meyer [57] showed that consistent results were obtained for the masses of the tensor and scalar glueballs from the different glueball calculations [2, 3, 25, 55], if r_0 was always used to determine the

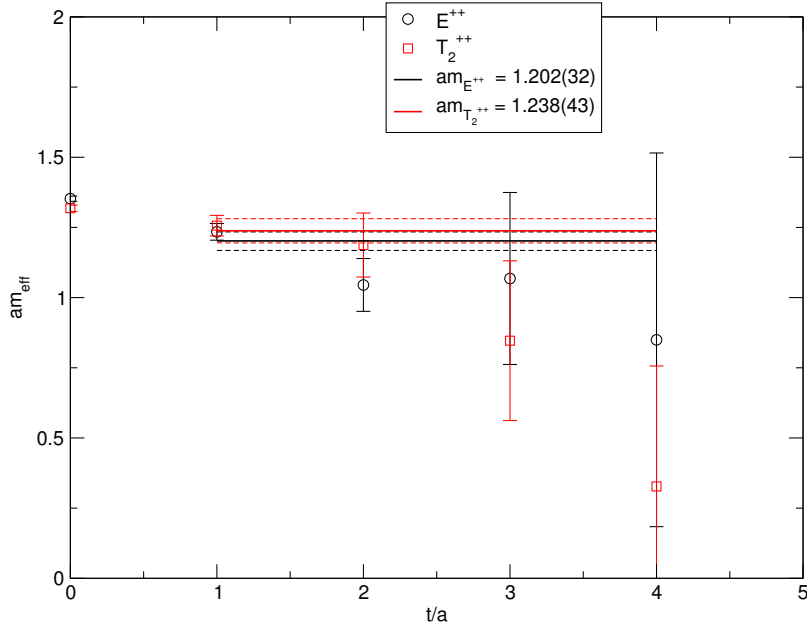


Figure 7. The ground state effective mass in the E^{++} channel is compared to the one in the T_2^{++} channel. These channels correspond to the continuum spin $J = 2$ representation and are supposed to be degenerate when the complete rotational symmetry is restored.

lattice spacing. In Fig. 8 we plot the summary of the glueball masses.

To compare with experiment we use the masses in the PDG. However we also include the additional masses reported by the Crystal Barrel collaboration, reviewed by Bugg [61]. Note that the Crystal Barrel experiment could only find new states in a restricted mass range. As explained in [60], some of the results from Anisovich et al. [58–60] are not included in the PDG summary tables, because they are neither confirmed nor excluded by other experiments. We plot the results for $I = 0$ mesons in [58, 59], but plot the 2^{++} states from [60]. These additional meson states from Anisovich et al. [58–60] have been used to find some experimental glueball candidates [62] from the quenched calculations of Morningstar and Peardon.

Bali [63] has plotted the quenched glueball spectrum with the experimental masses of the charmonium system.

5 Conclusions and future prospects

The most conservative interpretation of our results is that the masses in terms of lattice representations are broadly consistent with results from quenched QCD. We do not see any evidence for large unquenching effects, however a definitive calculation requires a continuum extrapolation, and the inclusion of fermionic operators. In Tab. 8 we tentatively assign J^{PC} quantum numbers to 10 glueballs.

Of particular note in Tab. 4 is that Meyer and Teper [25] do not see the two spin exotic states identified by Morningstar and Peardon [2]. In their summary of the glueball

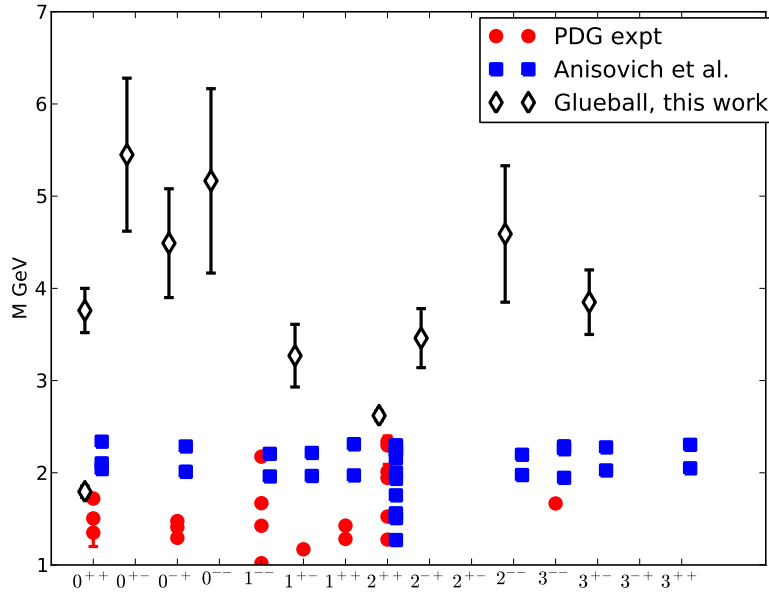


Figure 8. Summary of the glueball masses compared to experimental meson masses. The experimental results are from the PDG [29] and from Anisovich et al. [58–60].

spectrum Morningstar and Peardon note that their spin exotic glueball 2^{+-} could actually be part of 5^{+-} , 7^{+-} , or 11^{+-} glueball. Mathieu [42] have also compared the results for glueball masses from Morningstar and Peardon with those from Teper and Meyer. Our result for the mass of the 0^{+-} are consistent with the result from Morningstar and Peardon [2], although our errors are large for this heavy state. Meyer and Teper[4, 25] used sophisticated measurement techniques to help assign J^{PC} quantum numbers to their results in terms of lattice representations, but other groups reporting glueball masses have not done this. Given the importance of the masses of the oddball glueballs to the experimental program of PANDA, this issue needs to be resolved. Future lattice QCD calculations using heavy glueball degrees of freedom should use improved techniques to assign J^{PC} quantum numbers [4–6].

It would be advantageous to lattice QCD calculations if there were no light mesons above 3.1 GeV, because this would reduce the complicated mixing of glue and quark degrees of freedom. Aesthetically, it would be better to find an isolated glueball, rather than have to determine the mixture of glueball and quark degrees of freedom in a state such as the $f_0(1790)$. The determination of glueballs with exotic J^{PC} may be easier for lattice QCD calculations, although there is still the problem of the heavy mass and the poor signal to noise ratio.

Unquenched glueball calculations require much higher statistics than for the majority of flavour non-singlet lattice QCD calculations. We can use the numbers in Tab. 4 to estimate

roughly the number of configurations required to achieve a given accuracy. The most interesting states in Tab. 4 are the ones with exotic $J^{PC} = 0^{+-}$ and 2^{+-} quantum numbers. Using simple $1/\sqrt{N_{\text{configs}}}$ scaling, we can estimate that we need 550,000 configurations to get 50 MeV errors for the spin exotic 0^{+-} glueball.

The MILC collaboration has reported time estimates to produce ensembles of gauge configurations with 2+1+1 flavours of sea quarks with the HISQ improved staggered action. With the light quark a tenth of the strange quark mass, they estimate the time to generate 1000 configurations as 35, 128, and 352 Million core hours for the lattice spacings of: 0.09, 0.06, and 0.045 fm respectively². These numbers suggest that it is still too expensive to reduce the errors on the masses of the oddball glueballs. Lattice QCD calculations that use anisotropic lattices may be computationally cheaper.

The heavy glueballs may mix with charmonium states. To study this type of mixing will probably require both charm loops in the sea and the computation of disconnected diagrams [64, 65] for the charmonium valence states. There are a number of lattice QCD calculations, such as the one by the MILC collaboration [66], that include the dynamics of the charm quarks in the sea.

It is an exciting time for lattice QCD, with some unquenched lattice QCD calculations done with physical quark masses, and many unquenched calculations resulting in errors at the $O(1\%)$ level. The progress on lattice QCD calculations of glueballs is slower. However, the start of the PANDA experiment in 2018 provides an important deadline for lattice QCD calculations of glueballs.

Acknowledgments

The calculations were performed on the Liverpool cluster that is part of DiRAC funded by STFC. The gauge configurations were generated on the QCDOC [67]. We used Chroma [68] to make fermionic measurements. The work of B.L. is supported by the Royal Society and by STFC. ER is supported by a SUPA prize studentship and a JSPS short-term fellowship.

References

- [1] UKQCD Collaboration, G. Bali et al., *A Comprehensive lattice study of $SU(3)$ glueballs*, *Phys.Lett.* **B309** (1993) 378–384, [[hep-lat/9304012](#)].
- [2] C. J. Morningstar and M. J. Peardon, *The glueball spectrum from an anisotropic lattice study*, *Phys. Rev.* **D60** (1999) 034509, [[hep-lat/9901004](#)].
- [3] Y. Chen et al., *Glueball spectrum and matrix elements on anisotropic lattices*, *Phys. Rev.* **D73** (2006) 014516, [[hep-lat/0510074](#)].
- [4] H. B. Meyer and M. J. Teper, *Glueball Regge trajectories and the pomeron: A Lattice study*, *Phys.Lett.* **B605** (2005) 344–354, [[hep-ph/0409183](#)].
- [5] H. B. Meyer, *The Yang-Mills spectrum from a two level algorithm*, *JHEP* **0401** (2004) 030, [[hep-lat/0312034](#)].

²Talk presented by Paul Mackenzie at May 2011 review of the lqcd project.

- [6] D. Q. Liu and J. M. Wu, *The First calculation for the mass of the ground 4^{++} glueball state on lattice*, *Mod.Phys.Lett.* **A17** (2002) 1419–1430, [[hep-lat/0105019](#)].
- [7] **TXL** Collaboration, G. S. Bali et al., *Static potentials and glueball masses from QCD simulations with Wilson sea quarks*, *Phys.Rev.* **D62** (2000) 054503, [[hep-lat/0003012](#)].
- [8] **UKQCD** Collaboration, A. Hart and M. Teper, *On the glueball spectrum in $O(a)$ improved lattice QCD*, *Phys.Rev.* **D65** (2002) 034502, [[hep-lat/0108022](#)].
- [9] **UKQCD** Collaboration, A. Hart, C. McNeile, C. Michael, and J. Pickavance, *A Lattice study of the masses of singlet 0^{++} mesons*, *Phys.Rev.* **D74** (2006) 114504, [[hep-lat/0608026](#)].
- [10] **UKQCD** Collaboration, C. M. Richards, A. C. Irving, E. B. Gregory, and C. McNeile, *Glueball mass measurements from improved staggered fermion simulations*, *Phys. Rev.* **D82** (2010) 034501, [[arXiv:1005.2473](#)].
- [11] M. Della Morte and L. Giusti, *A novel approach for computing glueball masses and matrix elements in Yang-Mills theories on the lattice*, *JHEP* **1105** (2011) 056, [[arXiv:1012.2562](#)].
- [12] H.-Y. Cheng, C.-K. Chua, and K.-F. Liu, *Scalar glueball, scalar quarkonia, and their mixing*, *Phys. Rev.* **D74** (2006) 094005, [[hep-ph/0607206](#)].
- [13] H.-Y. Cheng, H.-n. Li, and K.-F. Liu, *Pseudoscalar glueball mass from eta - eta-prime - G mixing*, *Phys.Rev.* **D79** (2009) 014024, [[arXiv:0811.2577](#)].
- [14] G. Mennessier, S. Narison, and W. Ochs, *Glueball nature of the sigma/f0(600) from pi-pi and gamma-gamma scatterings*, *Phys. Lett.* **B665** (2008) 205–211, [[arXiv:0804.4452](#)].
- [15] F. E. Close and A. Kirk, *Scalar glueball q anti-q mixing above 1-GeV and implications for lattice QCD*, *Eur.Phys.J.* **C21** (2001) 531–543, [[hep-ph/0103173](#)].
- [16] W. Ochs, *No indication of f0(1370) in pi pi phase shift analyses*, *AIP Conf. Proc.* **1257** (2010) 252–256, [[arXiv:1001.4486](#)].
- [17] **CP-PACS** Collaboration, S. Aoki et al., *Lattice QCD Calculation of the rho Meson Decay Width*, *Phys.Rev.* **D76** (2007) 094506, [[arXiv:0708.3705](#)].
- [18] **ETM** Collaboration, K. Jansen, C. McNeile, C. Michael, and C. Urbach, *Meson masses and decay constants from unquenched lattice QCD*, *Phys.Rev.* **D80** (2009) 054510, [[arXiv:0906.4720](#)].
- [19] X. Feng, K. Jansen, and D. B. Renner, *Resonance Parameters of the rho-Meson from Lattice QCD*, *Phys.Rev.* **D83** (2011) 094505, [[arXiv:1011.5288](#)].
- [20] C. Lang, D. Mohler, S. Prelovsek, and M. Vidmar, *Coupled channel analysis of the rho meson decay in lattice QCD*, *Phys.Rev.* **D84** (2011) 054503, [[arXiv:1105.5636](#)].
- [21] S. Prelovsek, C. Lang, D. Mohler, and M. Vidmar, *Decay of rho and a1 mesons on the lattice using distillation*, *PoS LATTICE2011* (2011) 137, [[arXiv:1111.0409](#)].
- [22] D. Asner, T. Barnes, J. Bian, I. Bigi, N. Brambilla, et al., *Physics at BES-III*, *Int.J.Mod.Phys.* **A24** (2009) S1–794, [[arXiv:0809.1869](#)].
- [23] **BESIII** Collaboration, S. L. Olsen, *News from BESIII*, [arXiv:1203.4297](#).
- [24] **PANDA** Collaboration, M. Lutz et al., *Physics Performance Report for PANDA: Strong Interaction Studies with Antiprotons*, [arXiv:0903.3905](#).
- [25] H. B. Meyer, *Glueball Regge trajectories*, [hep-lat/0508002](#). Ph.D. Thesis.

- [26] M. M. Brisudova, L. Burakovsky, and J. Goldman, *Effective functional form of Regge trajectories*, *Phys.Rev.* **D61** (2000) 054013, [[hep-ph/9906293](#)].
- [27] P. R. Page, *Multi-GeV gluonic mesons*, [hep-ph/0107016](#).
- [28] E. S. Swanson, *Unquenching the quark model and screened potentials*, *J.Phys.G* **G31** (2005) 845–854, [[hep-ph/0504097](#)].
- [29] **Particle Data Group** Collaboration, K. Nakamura et al., *Review of particle physics*, *J.Phys.G* **G37** (2010) 075021.
- [30] J. J. Dudek et al., *Isoscalar meson spectroscopy from lattice QCD*, *Phys. Rev.* **D83** (2011) 111502, [[arXiv:1102.4299](#)].
- [31] R. Hagedorn, *Statistical thermodynamics of strong interactions at high-energies*, *Nuovo Cim.Suppl.* **3** (1965) 147–186.
- [32] R. Hagedorn, *Hadronic matter near the boiling point*, *Nuovo Cim.* **A56** (1968) 1027–1057.
- [33] T. D. Cohen and V. Krejvcivrik, *Does the empirical meson spectrum support the Hagedorn conjecture?*, [arXiv:1107.2130](#).
- [34] S. Chatterjee, R. M. Godbole, and S. Gupta, *Stabilizing hadron resonance gas models*, *Phys. Rev.* **C81** (2010) 044907, [[arXiv:0906.2523](#)].
- [35] S. Borsanyi, G. Endrodi, Z. Fodor, A. Jakovac, S. D. Katz, et al., *The QCD equation of state with dynamical quarks*, *JHEP* **1011** (2010) 077, [[arXiv:1007.2580](#)].
- [36] **Wuppertal-Budapest** Collaboration, S. Borsanyi et al., *Is there still any T_c mystery in lattice QCD? Results with physical masses in the continuum limit III*, *JHEP* **1009** (2010) 073, [[arXiv:1005.3508](#)].
- [37] A. Majumder and B. Muller, *Hadron Mass Spectrum from Lattice QCD*, *Phys.Rev.Lett.* **105** (2010) 252002, [[arXiv:1008.1747](#)].
- [38] E. Megias, E. R. Arriola, and L. Salcedo, *The hadron resonance gas model: thermodynamics of QCD and Polyakov loop*, [arXiv:1207.7287](#).
- [39] U. Wiedner, *Future Prospects for Hadron Physics at PANDA*, *Prog.Part.Nucl.Phys.* **66** (2011) 477–518, [[arXiv:1104.3961](#)].
- [40] B. Lucini, A. Rago, and E. Rinaldi, *Glueball masses in the large N limit*, *JHEP* **08** (2010) 119, [[arXiv:1007.3879](#)].
- [41] E. Klempt and A. Zaitsev, *Glueballs, Hybrids, Multiquarks. Experimental facts versus QCD inspired concepts*, *Phys.Rept.* **454** (2007) 1–202, [[arXiv:0708.4016](#)].
- [42] V. Mathieu, N. Kochelev, and V. Vento, *The Physics of Glueballs*, *Int. J. Mod. Phys.* **E18** (2009) 1–49, [[arXiv:0810.4453](#)].
- [43] C. McNeile, *Lattice status of gluonia/glueballs*, *Nucl.Phys.Proc.Suppl.* **186** (2009) 264–267, [[arXiv:0809.2561](#)].
- [44] V. Crede and C. A. Meyer, *The Experimental Status of Glueballs*, *Prog. Part. Nucl. Phys.* **63** (2009) 74–116, [[arXiv:0812.0600](#)].
- [45] **MILC** Collaboration, K. Orginos and D. Toussaint, *Testing improved actions for dynamical Kogut-Susskind quarks*, *Phys.Rev.* **D59** (1999) 014501, [[hep-lat/9805009](#)].
- [46] **MILC** Collaboration, K. Orginos, D. Toussaint, and R. Sugar, *Variants of fattening and flavor symmetry restoration*, *Phys.Rev.* **D60** (1999) 054503, [[hep-lat/9903032](#)].

- [47] M. G. Alford, W. Dimm, G. P. Lepage, G. Hockney, and P. B. Mackenzie, *Lattice QCD on small computers*, *Phys. Lett.* **B361** (1995) 87–94, [[hep-lat/9507010](#)].
- [48] A. Bazavov et al., *Full nonperturbative QCD simulations with 2+1 flavors of improved staggered quarks*, *Rev. Mod. Phys.* **82** (2010) 1349–1417, [[arXiv:0903.3598](#)].
- [49] E. B. Gregory, A. C. Irving, C. M. Richards, and C. McNeile, *A study of the eta and eta' mesons with improved staggered fermions*, *Phys.Rev.* **D86** (2012) 014504, [[arXiv:1112.4384](#)].
- [50] **HPQCD** Collaboration, C. Davies, E. Follana, I. Kendall, G. Lepage, and C. McNeile, *Precise determination of the lattice spacing in full lattice QCD*, *Phys.Rev.* **D81** (2010) 034506, [[arXiv:0910.1229](#)].
- [51] B. Lucini, M. Teper, and U. Wenger, *Glueballs and k-strings in SU(N) gauge theories: Calculations with improved operators*, *JHEP* **0406** (2004) 012, [[hep-lat/0404008](#)].
- [52] Z. Fu, *Preliminary lattice study of σ meson decay width*, *JHEP* **1207** (2012) 142, [[arXiv:1202.5834](#)].
- [53] V. Bernard, M. Lage, U.-G. Meissner, and A. Rusetsky, *Scalar mesons in a finite volume*, *JHEP* **1101** (2011) 019, [[arXiv:1010.6018](#)].
- [54] M. Doring, U. Meissner, E. Oset, and A. Rusetsky, *Scalar mesons moving in a finite volume and the role of partial wave mixing*, [[arXiv:1205.4838](#)].
- [55] H. B. Meyer and M. J. Teper, *High spin glueballs from the lattice*, *Nucl.Phys.* **B658** (2003) 113–155, [[hep-lat/0212026](#)].
- [56] J. J. Dudek, R. G. Edwards, N. Mathur, and D. G. Richards, *Charmonium excited state spectrum in lattice QCD*, *Phys.Rev.* **D77** (2008) 034501, [[arXiv:0707.4162](#)].
- [57] H. B. Meyer, *Glueball matrix elements: a lattice calculation and applications*, *Journal of High Energy Physics* **2009** (2008), no. 01 071, [[arXiv:0808.3151](#)].
- [58] A. Anisovich, C. Baker, C. Batty, D. Bugg, C. Hodd, et al., *$I = 0$ $C = +1$ mesons from 1920 to 2410 MeV*, *Phys.Lett.* **B491** (2000) 47, [[arXiv:1109.0883](#)].
- [59] A. Anisovich, C. Baker, C. Batty, D. Bugg, L. Montanet, et al., *$I=0$, $C=-1$ mesons from 1940 to 2410 MeV*, *Phys.Lett.* **B542** (2002) 19, [[arXiv:1109.5817](#)].
- [60] A. Anisovich, D. Bugg, V. Nikonov, A. Sarantsev, and V. Sarantsev, *Light 2^{++} and 0^{++} mesons*, *Phys.Rev.* **D85** (2012) 014001, [[arXiv:1110.4333](#)].
- [61] D. V. Bugg, *Four Sorts of Mesons*, *Phys. Rept.* **397** (2004) 257–358, [[hep-ex/0412045](#)].
- [62] D. Bugg, M. J. Peardon, and B. Zou, *The Glueball spectrum*, *Phys.Lett.* **B486** (2000) 49–53, [[hep-ph/0006179](#)].
- [63] G. S. Bali, *Charmonia from lattice QCD*, *Int.J.Mod.Phys.* **A21** (2006) 5610–5617, [[hep-lat/0608004](#)]. 8 pages, 5 figures, Invited talk presented at “Charm 2006”, Beijing, 5-7 June 2006.
- [64] **UKQCD** Collaboration, C. McNeile and C. Michael, *An Estimate of the flavor singlet contributions to the hyperfine splitting in charmonium*, *Phys.Rev.* **D70** (2004) 034506, [[hep-lat/0402012](#)].
- [65] L. Levkova and C. DeTar, *Charm annihilation effects on the hyperfine splitting in charmonium*, *Phys.Rev.* **D83** (2011) 074504, [[arXiv:1012.1837](#)].

- [66] **MILC** Collaboration, A. Bazavov et al., *Scaling studies of QCD with the dynamical HISQ action*, *Phys.Rev.* **D82** (2010) 074501, [[arXiv:1004.0342](#)].
- [67] P. Boyle, D. Chen, N. Christ, M. Clark, S. D. Cohen, et al., *The QCDOC project*, *Nucl.Phys.Proc.Suppl.* **140** (2005) 169–175.
- [68] **SciDAC, LHPC, UKQCD** Collaboration, R. G. Edwards and B. Joo, *The Chroma software system for lattice QCD*, *Nucl.Phys.Proc.Suppl.* **140** (2005) 832, [[hep-lat/0409003](#)].